CONV-22

5th International Symposium on Convective Heat and Mass Transfer

Izmir, Turkey, June 5 - 10, 2022

Computer modelling of thermally-driven microclimate phenomena

Kemal (Kemo) Hanjalić

Delft University of Technology, Nl

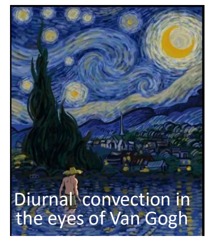

Diurnal convection in the eyes of Van Gogh

Contributed by

Michael Hrebtov (NSU) and Saša Kenjereš (TUD)

TUDelft Delft University of Technology

ICHMT Luikov Medal Lecture

Novosibirsk State University

Winter scenes over large rivers / lakes in cold climate

Wavy fog pattern and 'steam devils'

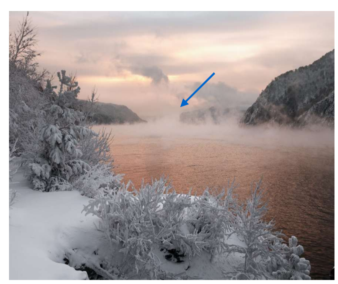

http://raskalov-it.livejournal.com/122977.html

(Balme & Greeley, 2006)

2

Geophysical Flows: RANS, LES, HRL *

- Just as in general CFD, two strategies prevail in the computation of Geophysical flows: (U)RANS and LES, (few Hybrid, if any?)
- RANS prevails in practical applications (wind engineering, pollutant dispersion,..), most often steady, standard two-eqn LEVM+SWF
- LES dominant among the atmospheric community ("Turbulence models cannot serve as a predictive tool" (?), *Wyngaard, 1992*)
- Most LES: regular domains over a flat terrain, (several kms), very fine meshes (O 10^7-10^9), Monin-Obukhov scaling for ground conditions
- *Coarse* LES can capture dominant structures ("wind") in outer CBL, but hardly credible for resolving ground layer over real orography.
- URANS (ensemble averaged): option for *real-scales and coarse mesh;* captures large-scales, easier to account for "subscales" and GBC.

*RANS: Reynolds-averaged Navier-Stokes; LES Large-eddy simulations; HRL: hybrid 3

Comprehensive Set of Test Cases for Natural Convection

		Type of Flow Experiment/DNS/LES	$k-\varepsilon$ SGDH	$k-\varepsilon$ GGDH	AFM k-ε-θ^2	AFM k-ε-θ^2-ε_θ	DFM
1		Heated vertical plate Exp: Tsuji & Nagano (1988)	X	X	X	X	X
2		Vertical channel, tall cavities (30:1) Exp: Betts & Dafa' Alla (1986) DNS: Boudjemadi /em et al.(1997) DNS: Versteegh & Nieuwstadt (1997)	X	X	X	X	X
3	T	Penetrative convection of mixed layer above heated horizontal wall Exp: Deardorff et al. (1969)				X	X
4		Rayleigh-Bénard convection Exp: Chu & Goldstein (1973) DNS: Grötzbach (1982), Kerr(1996) Balachandar *et al.* (1989), Wörner (1994)	X	X	X	X	
5	T_h T_c	Side heated vertical cavities (1:1, 5:1) Exp: Cheesewright et al. (1986-90)	X	X	X	X	X
6	T_h T_c T_b(or q=0)	Square cavities with mixed boundary conditions Exp: Kirkpatrick & Bohn (1986)	X	X	X		
7	T_h T_c	Shallow cavities heated from side Exp: Olson et al. (1:2, 1:3) (1990)	X		X		
8	T_c T_h	Partitioned multi-zone cavities with mixed boundary conditions Exp:	X				
9	T_h T_c	Cavities with partial division Exp: Nansteel & Greif (1984), Olson et al. (1990)	X	X	X		
10	T_h T_c	Horizontal concentric annuli Exp: Kuehn & Goldstein (1978), Mcleod & Bishop (1989) LES: Miki et al. (1993)	X	X	X		
11	T_h T_c	Horizontal eccentric annuli Exp: Kuehn & Goldstein (1978)			X		
12		Side heated cubic enclosure Exp:			X		X

Legend:
SGDH – Simple Gradient Diffusion Hypothesis. (isotropic eddy diffusivity)
GGDH – Generalized Gradient Diffusion (non-isotropic eddy diffusivity)
AFM — Algebraic Flux Model
DFM — Differential Flux Model

TUDelft Delft University of Technology 2004

Thermal convection: regimes and solution accessibility

(Rayleigh-Bénard, Penetrative convection,…)

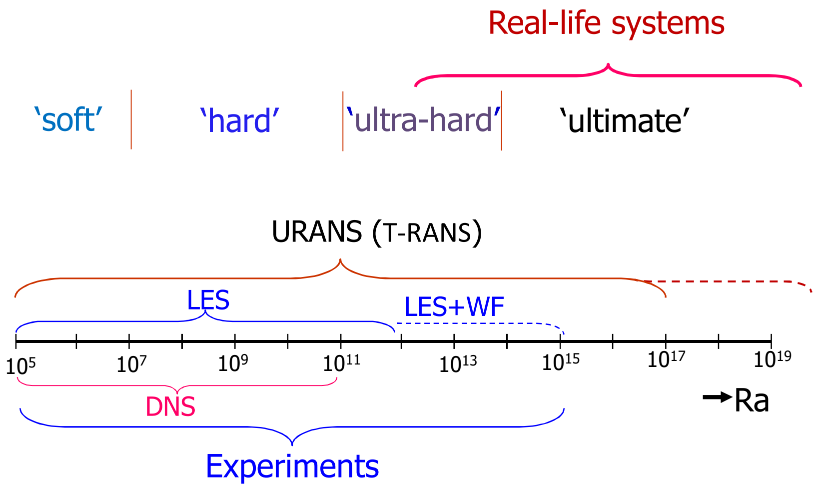

5

High-Ra number challenges:

R-B & penetrative thermal convection

- Nu $\propto$ $Ra^{1/3}$ for $Ra<10^{12}$ *(Pr $\mathcal{O}(1)$)*
- Nu $\propto$ $Ra^{1/2}$ for Ra $\to\infty$ (*Kraichnan*)
- $\lambda_v/H \propto Ra^{-1/7}$
- $\lambda_\theta/H \propto Ra^{-1/3}$

For high Ra, Wall-layer resolving prohibitive!

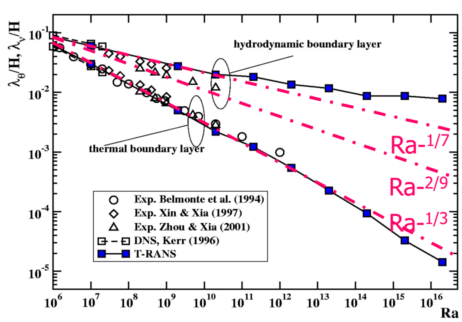

Thicknesses of thermal and hydrodynamic b.l. vs Ra (*Kenjereš & Hanjalić, 2006, 2009*).

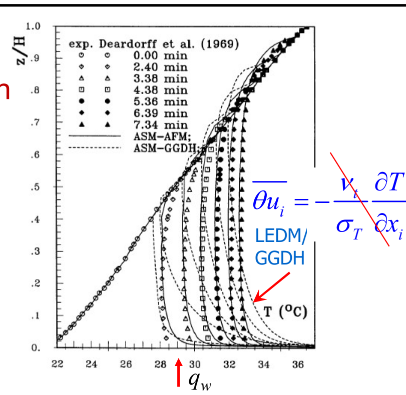

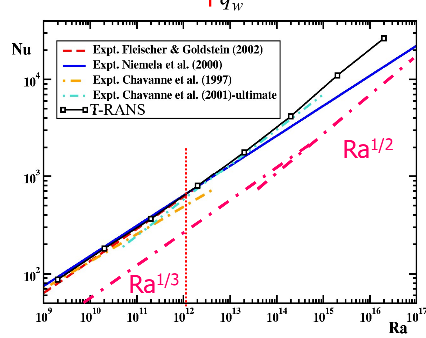

6

T-RANS: Time-resolved ensemble-averaged RANS*

A time record of the instantaneous and *locally* time-averaged velocity in a flow with organised (periodic, coherent) large-scale structures

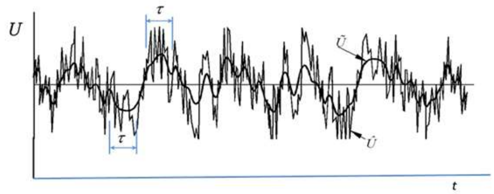

$$\hat{\Phi} = \tilde{\Phi} + \varphi$$

$$\tilde{\Phi}(x_i, t) = \frac{1}{\tau} \int_{t-\tau/2}^{t+\tau/2} \hat{\Phi}(x_i, t)\, dt$$

Triple decomposition:

$$\hat{\Phi}(x_i,t) = \underbrace{\underbrace{\overline{\Phi}(x_i)}_{mean} + \underbrace{\varphi^c(x_i,t)}_{periodic}}_{phase-averaged} + \underbrace{\varphi^s(x_i,t)}_{stochastic}$$

;

$$\overline{\hat{\Phi}\hat{\Psi}} = \overline{\overline{\Phi}}\,\overline{\overline{\Psi}} + \overline{\varphi^c\psi^c} + \cancel{\overline{\varphi^c\psi^s}} + \cancel{\overline{\varphi^s\psi^c}} + \overline{\varphi^s\psi^s}$$

Scales separation $\mathcal{T}^c >> \mathcal{T}^s$

Effective second moments:

$$\boxed{\overline{\hat{\Phi}\hat{\Psi}} - \overline{\Phi}\,\overline{\Psi} = \underbrace{\overline{\varphi^c\psi^c}}_{resolved} + \underbrace{\overline{\varphi^s\psi^s}}_{modelled}}$$

*T-RANS: the standard URANS equations, just the matter of interpretation, provided the time step is small enough to resolve coherent motion!

(Kenjereš & Hanjalić 1999). 7

Governing equations and turbulence model for T-RANS

- Ensemble-averaged equations (<>) for momentum, energy and humidity:

$$\frac{D\langle U_i\rangle}{Dt} = -\frac{\partial\langle u_i u_j\rangle}{\partial x_i} - \frac{1}{\rho}\frac{\partial\langle P\rangle}{\partial x_i} + \beta_T g_i\left(\langle T\rangle - T_{ref}\right) - \beta_H g_i\left(\langle H\rangle - H_{ref}\right)$$

$$\frac{D\langle T\rangle}{Dt} = -\frac{\partial\langle\theta u_i\rangle}{\partial x_i}; \quad \frac{D\langle H\rangle}{Dt} = -\frac{\partial\langle h u_i\rangle}{\partial x_i}; \quad \beta_T = -\frac{1}{\rho_0}\left(\frac{\partial\rho}{\partial T}\right)_{H,p}; \quad \beta_H = \frac{1}{\rho_0}\left(\frac{\partial\rho}{\partial H}\right)_{T,p}$$

- Turbulence closure: "reduced" algebraic stress/flux model (*ASM/AFM* k-ε-θ^2)

$$\langle u_i u_j\rangle = -\upsilon_t\left(\frac{\partial\langle U_i\rangle}{\partial x_j} + \frac{\partial\langle U_j\rangle}{\partial x_i}\right) + \frac{2}{3}\langle k\rangle\delta_{ij} -$$

$$\Rightarrow \quad -c_\phi\frac{\langle k\rangle}{\langle\varepsilon\rangle}\left[\beta_T\left(g_i\langle\theta u_j\rangle + g_j\langle\theta u_i\rangle\right) - \beta_H\left(g_i\langle h u_j\rangle + g_j\langle h u_i\rangle\right)\right]$$

$$\Rightarrow \quad \langle\theta u_i\rangle = -c_\phi\frac{\langle k\rangle}{\langle\varepsilon\rangle}\left(\langle u_i u_j\rangle\frac{\partial\langle T\rangle}{\partial x_j} + \xi\langle\theta u_j\rangle\frac{\partial\langle U_i\rangle}{\partial x_j} + \eta\beta_T g_i\langle\theta^2\rangle + \varsigma\beta_h g_i\langle\theta h\rangle\right)$$

$$\langle h u_i\rangle = -c_\phi\frac{\langle k\rangle}{\langle\varepsilon\rangle}\left(\langle u_i u_j\rangle\frac{\partial\langle H\rangle}{\partial x_j} + \xi\langle h u_i\rangle\frac{\partial\langle U_i\rangle}{\partial x_j} + \eta\beta_H g_i\langle h^2\rangle + \varsigma\beta_H g_i\langle\theta h\rangle\right)$$

8

Turbulence model, cont.: the 3–eqn model

$$\frac{D\langle k\rangle}{Dt}=\mathcal{D}_k+\mathcal{P}_k+\mathcal{G}_k-\langle\varepsilon\rangle;\quad \frac{D\langle\varepsilon\rangle}{Dt}=\mathcal{D}_\varepsilon+\mathcal{P}_\varepsilon+\mathcal{G}_\varepsilon-Y;\quad \frac{D\langle\theta^2\rangle}{Dt}=\mathcal{D}_\theta+\mathcal{P}_\theta-\langle\varepsilon_\theta\rangle;$$

$$\mathcal{P}_k=-\langle u_iu_j\rangle\frac{\partial\langle U_i\rangle}{\partial x_j};\quad \mathcal{G}_k=-\beta g_i\langle\theta u_i\rangle;\quad \mathcal{P}_\theta=-\langle\theta u_j\rangle\frac{\partial\langle T\rangle}{\partial x_j};\quad \langle\varepsilon_\theta\rangle=\langle\varepsilon\rangle\frac{\langle\theta^2\rangle}{\langle k\rangle}$$

$$\mathcal{D}_\phi=\frac{\partial}{\partial x_j}\left(\frac{\nu_t}{\sigma_\phi}\frac{\partial\langle\phi\rangle}{\partial x_j}\right);\quad \mathcal{P}_\varepsilon=C_{\varepsilon1}\frac{\mathcal{P}_k\langle\varepsilon\rangle}{\langle k\rangle};\quad \mathcal{G}_\varepsilon=C_{\varepsilon3}\frac{\mathcal{G}_k\langle\varepsilon\rangle}{\langle k\rangle};\quad Y=C_{\varepsilon2}\frac{\langle\varepsilon\rangle^2}{\langle k\rangle};$$

Validation of the model (with wall-integration) in R-B convection for Ra=10^5-10^{16}

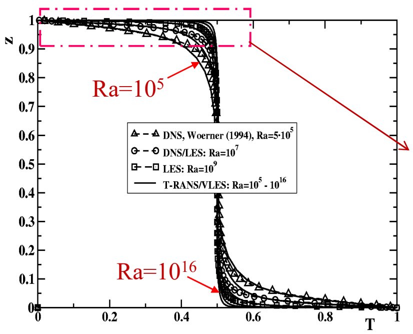

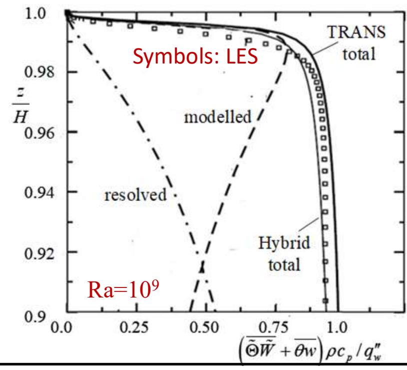

(Kenjereš & Hanjalić, 1999, 2006)

9

Buoyancy-accounting NE Ground/Wall Functions

- Ground surface stress and heat flux

$$\tau_s=\mu_s^{eff}\frac{U_P-U_s}{z_P};\quad q_s=\alpha_s^{eff}\frac{T_P-T_s}{z_P};\quad \mu_s^{eff}=\frac{\psi\kappa^*\rho k_P^{1/2}z_P}{\ln(E^*z_P^*)};\quad \alpha_s^{eff}=\frac{\psi_\Theta\tilde{\kappa}^*k_P^{1/2}z_P}{\ln(\tilde{E}^*z_P^*)}$$

- Accounting for non-equilibrium effects (SAWF):

$$\psi=1-\frac{C_Uz_P}{\rho\kappa c_\mu^{1/4}k_P^{1/2}U_P}=1-\frac{C_U^*z_P^*}{\kappa^*U_P^*}\qquad \psi_\Theta\equiv1-\frac{\sigma_\Theta C_\Theta y_P}{\rho c_p\kappa\sqrt{\tau_s/\rho}\,(T_P-T_w)}=1-\frac{\sigma_\Theta C_\Theta^*y_P^*}{\kappa\Theta_P^*}$$

$$C_U^*=\frac{C_U\mu}{\rho k_P^{1/2}\tau_s}=\frac{\mu}{\rho k_P^{1/2}\tau_s}\left(\rho\frac{\partial U}{\partial t}+\rho U\frac{\partial U}{\partial x}+\rho V\frac{\partial U}{\partial y}+\frac{dP}{dx}-\rho_0g_3\beta(T-T_0)\right)_P$$

$$C_\Theta^*=\frac{\mu}{\rho c_\mu^{1/4}k_P^{1/2}q_s}\left[\rho c_p\frac{\partial T}{\partial t}+\rho c_pU\frac{\partial T}{\partial x}+\rho c_pV\frac{\partial T}{\partial y}+S_\Theta\right]_P$$

- Humidity (in terms of saturation pressure)

$$\left.\begin{aligned}H&=\frac{2.1667\,p_w}{273.15+T}\\ p_w(T,H)&=611.2e^{17.62T/(243.12+T)}\end{aligned}\right\}\quad H_P=\frac{1323.9\,e^{17.62T_P/(243.17+T_P)}}{273.15+T_P}$$

(Hanjalic and Hrebtov, Bound. Layer Meteor. 2016)

10

Validation of Ground boundary functions (SAGF)

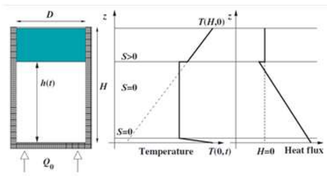

$$\mathcal{P}_{k\,\mathrm{P}} = \frac{U_\tau^2 c_\mu^{1/4} k_\mathrm{P}^{1/2}}{\psi \kappa z_\mathrm{P}} \qquad \mathcal{G}_{k,\mathrm{P}} = \beta g_i \sqrt{q_{s,i}} \left(c_{\mu,\theta}^{1/2} \sqrt{\theta_\mathrm{P}^2 k_\mathrm{P}} \right)^{1/2}$$

$$\varepsilon_\mathrm{P} = \frac{c_\mu^{3/4} k_\mathrm{P}^{3/2}}{\kappa z_\mathrm{P}} \qquad \mathcal{P}_{\theta,\mathrm{P}} = \frac{q_s c_{\mu,\theta}^{1/2} \sqrt{\overline{\theta^2}_\mathrm{P}}}{\psi_\Theta \tilde{\kappa}^* z_\mathrm{P}} \qquad \varepsilon_{\theta,\mathrm{P}} = 2\varepsilon_\mathrm{P} \frac{\overline{\theta^2}_\mathrm{P}}{k_\mathrm{P}}$$

Penetrative convection (Exp. *Deardorff et al*. 1969}

Grid: 10×10×100 (N_x×N_y×N_z)

Grid: 10×10×**20**

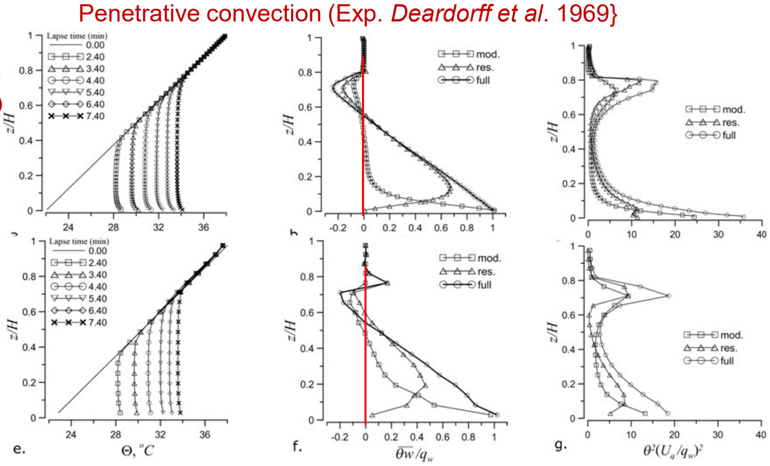

11

Time evolution of the penetrative mixed layer heated from below

Short-time filtered T-RANS velocity (colours: vertical velocity) , SAGF

Grid 40×40×100 ,
domain 2:2:1

Grid 10 × 10 × 100,
domain 1:1:1

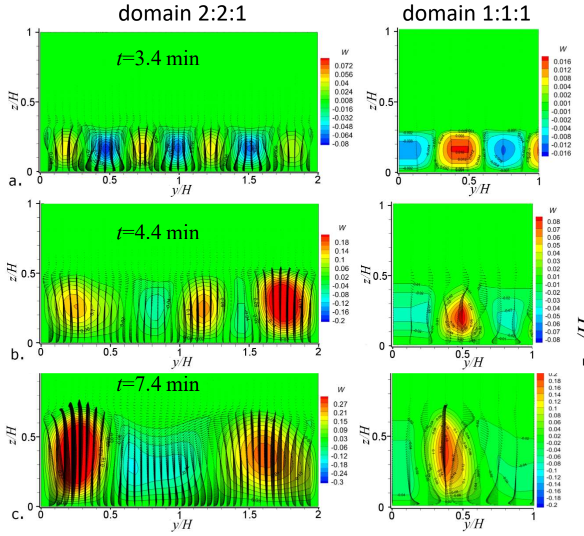

Mixed layer height $h(\equiv z_{inv})$
(at max. negative heat flux)

$h \propto \sqrt{t}$ *(Fedorovich et al, 1994)*

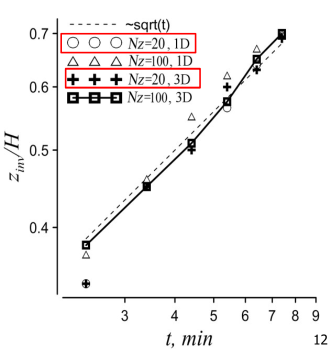

12

Further T-RANS validations: Cellular pattern of sheet-like plumes

T-RANS R-B conv
Ra=10^9 z/H=0.005
Grid: 0.5×10^6
(*Kenjereš & Hanjalić, 2006*).

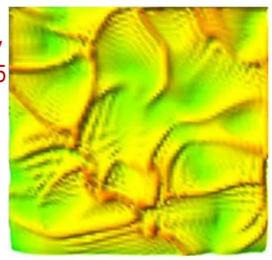

Isosurface of T=const coloured by vertical velocity in R-B convection,

Morning in Sahara – sand cats' paws

13

REAL Case: Krasnoyarsk winter scenario, Ra~10^{18} (T-RANS)

Terrain: mildly hilly, max height ~400 m
Ground (equiv.) roughness: 3 zones:
5m – city, 1 m – surrounding, 0.1m - river

Domain $32\times17\times2$ km,
Grid: 322x172x102 (~5.6 mil cells)

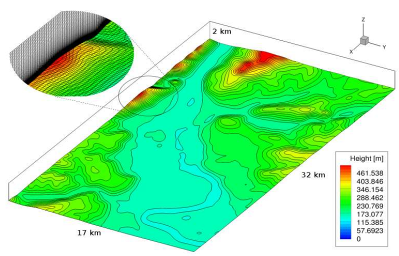

2d simulation of the river surface movement,
Mean speed 4 m/s
Temperature 0°C

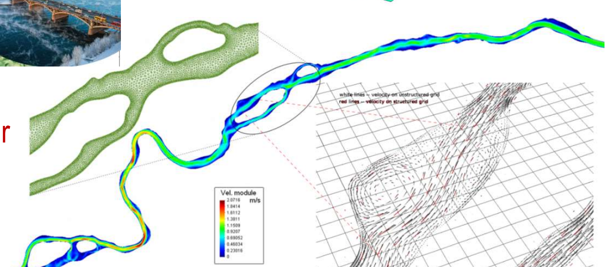

(Hrebtov & Hanjalić, 2017)

14

Ground temperature distribution at different diurnal phases

Measurements at two stations, z=2m, Febr. 2016, 6 days

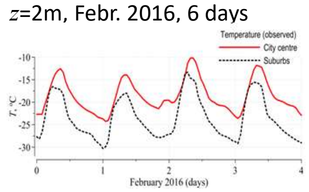

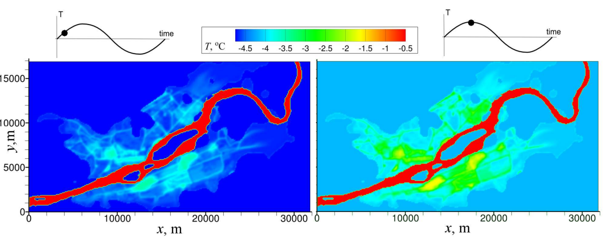

Plane averaged temperature and heat-flux profiles for different diurnal phases

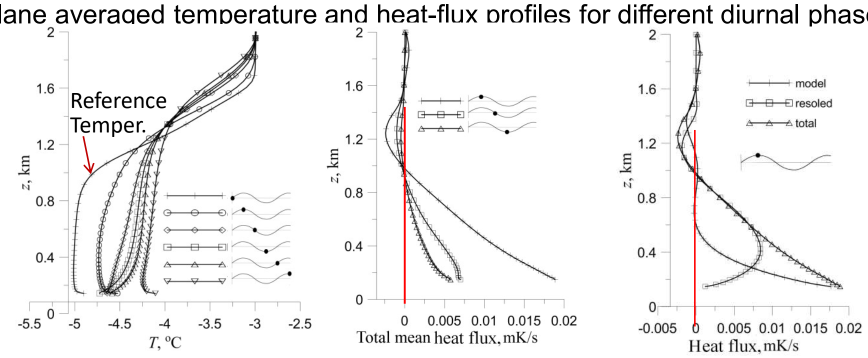

15

Temperature (a) and heat flux (b) profiles integrated over a local 1×1 km square area at three characteristic phases (noon, sunset and midnight).

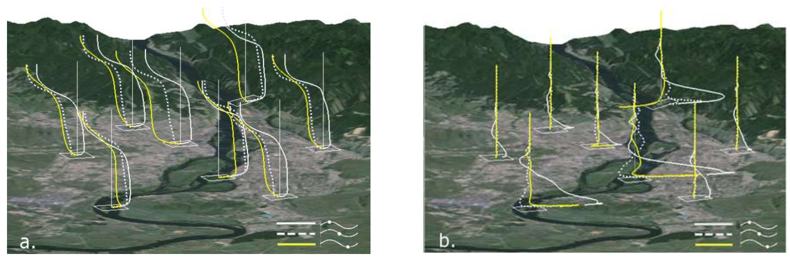

Heat flux and its resolved and modelled constituents for noon and midnight

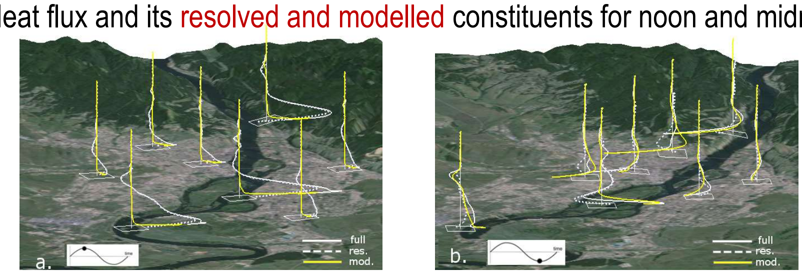

16

Illustration of T-RANS resolution of dominant large scales

The y-comp. of the horizontal velocity at 50 m above the ground at 24:00 and 12:00 h

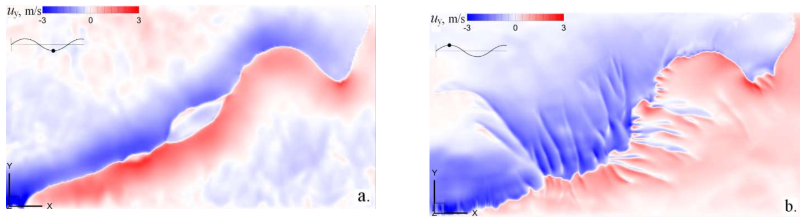

Stream lines in a selected vertical cross section normal to the river

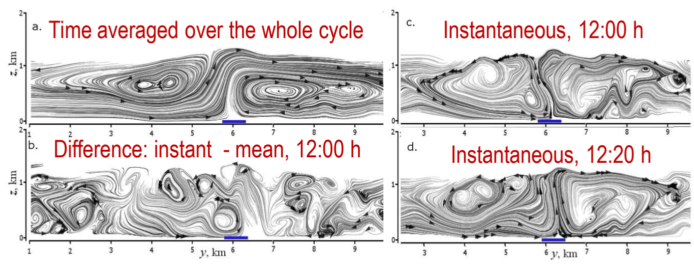

17

Temperature and humidity with velocity vector projections

at 18:00 hr in river-normal cross-sections over and around river branching

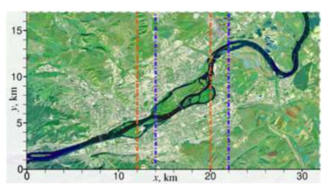

Temperature field

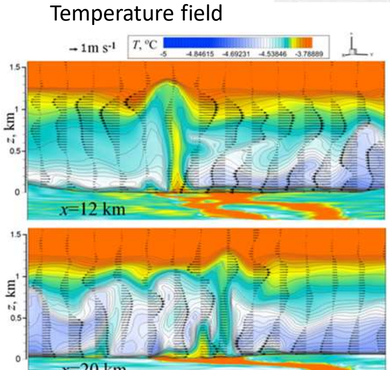

River

Water vapour contours

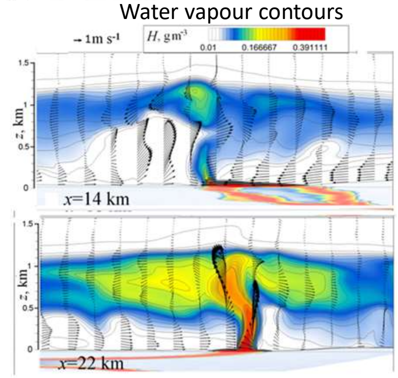

Hrebtov & Hanjalić (2017)

18

Undulating fog pattern (vapour concentration)

Translucent volume rendering

Horizontal planes

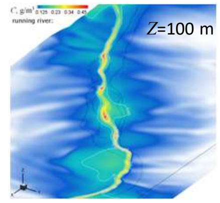

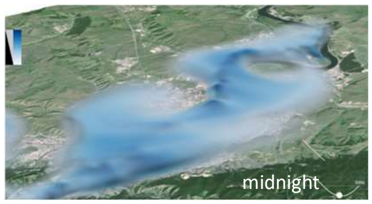

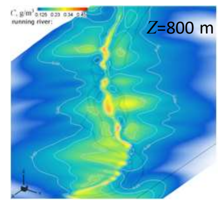

19

VORTICAL STRUCTURES, Q criterion, coloured by helicity $(u_i \omega_i)$

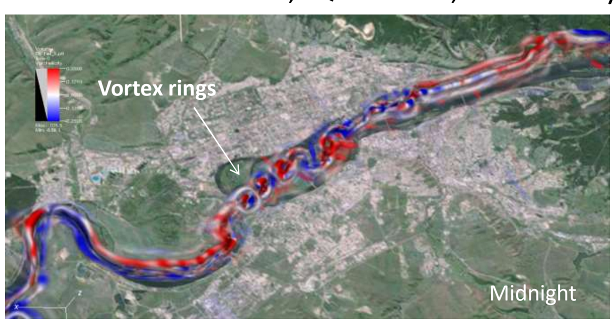

River-parallel counter-rotating vortices

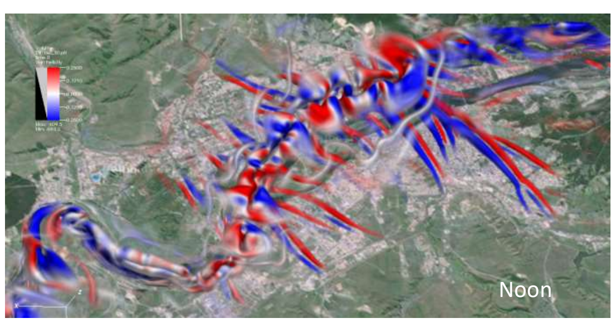

River-normal counter-rotating 'trumpet'- like vortices

20

River-parallel vorticity generation by the horizontal temp. gradient

River-parallel vorticity component with the low-pass-filtered temperature distribution along the ground-adjacent computational points.

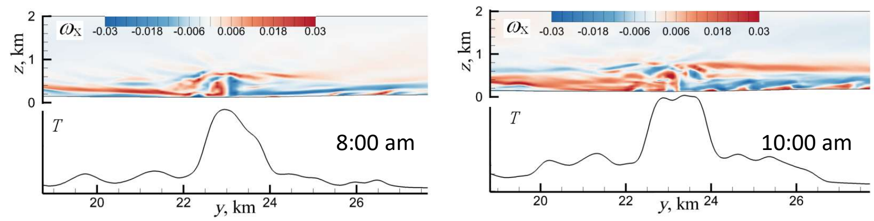

$$\frac{D\vec{\omega}}{Dt} = \ldots + \nabla(\beta T)\times\vec{g}$$ (Baroclinic vorticity generation)

River-normal streaks generation?

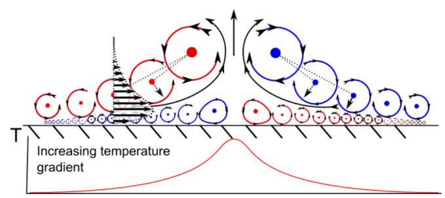

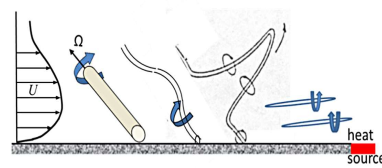

Formation of ‘dust-devil’ in stable CBL: High-resolution LES

Kanak 2005, Raasch & Franke 2011, Rafkin et al 2016, Spiga et al 2016, Onishchenko et al. 2019 Giersch & S. Raasch 2021

Honeycomb structure and vorticity-generating mechanisms near the flat surface of a CBL (heated from below).

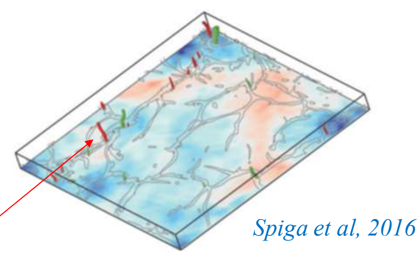

4x4x1.7 km, 10^9 grid cells

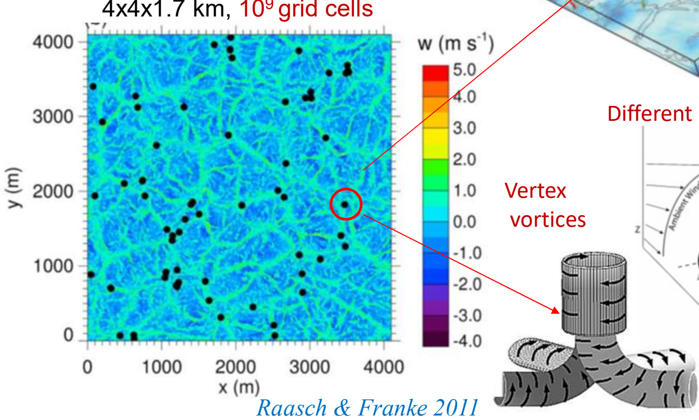

Different mechanism in wind-shear

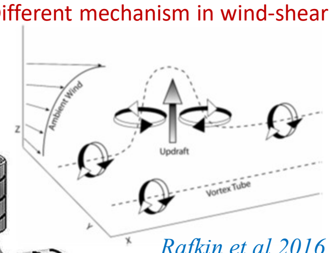

Krasnoyarsk: Vertical vorticity at 20m alt.; T-RANS 5.6 mill cells

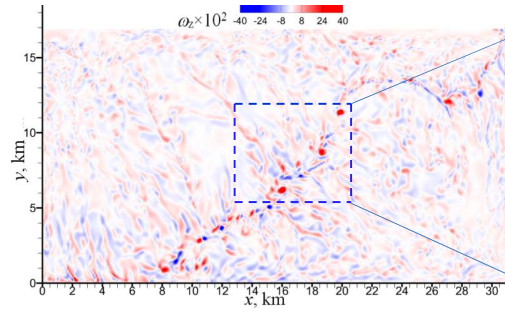

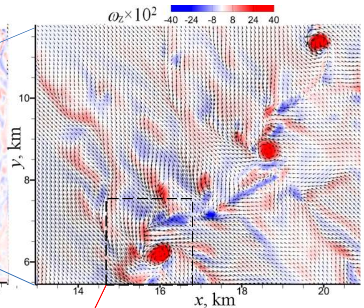

“Steam devil” over the river at 12.00 hr, visualised by streamlines

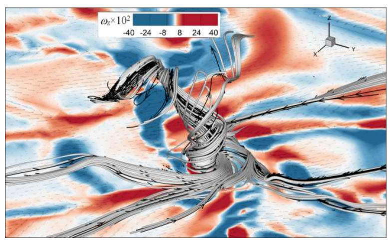
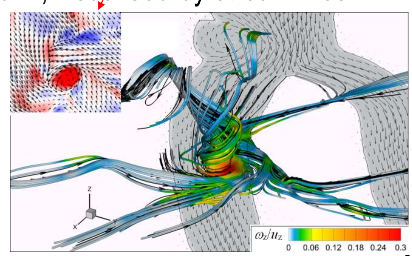

Colours: vertical vorticity at 20 m altitude

23

‘Steam devils’ - columnar spiralling structures over a lake/river at $T_s > T_a$, typically 50 to 200 m in diameter, up to 500 m high…

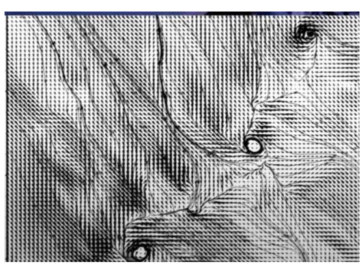


Feb 10, 2014 Clinton lake, IL steam devils

https://youtu.be/hWOP3u_m9xQ ;

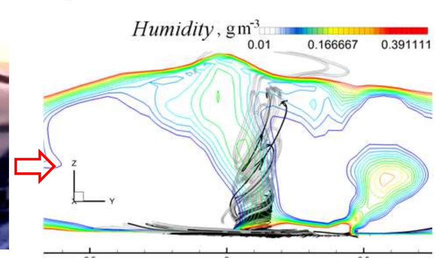

(Hrebtov & Hanjalić, 2017)

24

The role of river in different seasons
Summer: heat sink; Winter: heat source

Instantaneous vortex structure over the city educted by the Q-criterion, colored by temperature

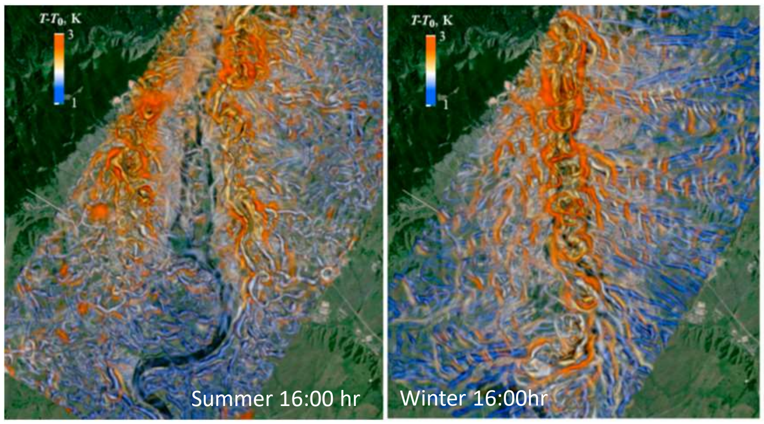

(Hrebtov & Hanjalić, Atmosphere, 2019)

25

River-induced anomalies in seasonal variation of traffic-emitted CO distribution over the City of Krasnoyarsk

Instantaneous and daily averaged CO in horizontal planes at 50 m height

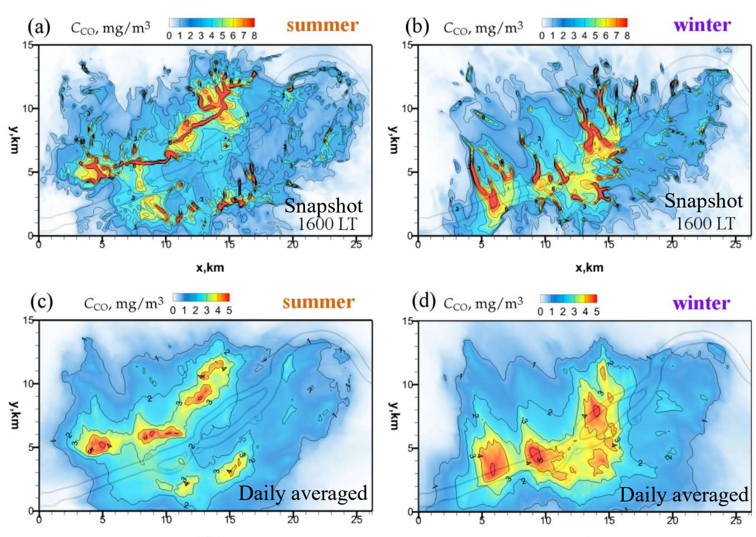

26

Pollutant (CO) concentration dispersion – winter diurnal cycle

Snapshots of instantaneous CO concentration at 18:00 hr

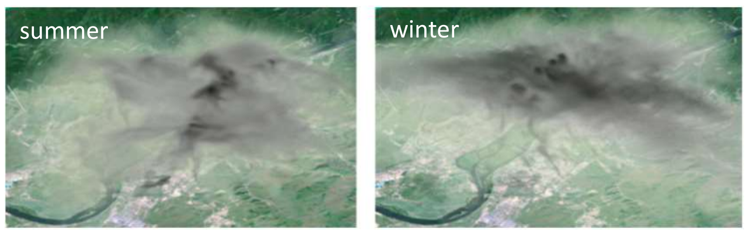

27

CO distribution over the City of Krasnoyarsk

Comparison of the measured and simulated CO concentrations.
(daily averages at various locations).

E.g. at #4, CO_{max}:
Winter: measured: 7.2 mg/m^3
computed: 6.9 mg/m^3
Summer: measured : 4.5 mg/m^3
computed: 3.1 mg/m^3

Measuring stations, 10m above the ground

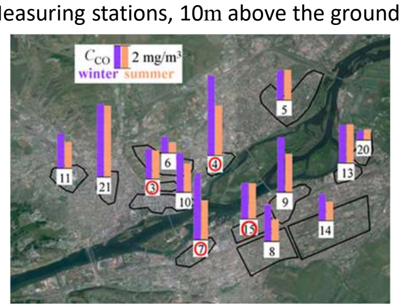

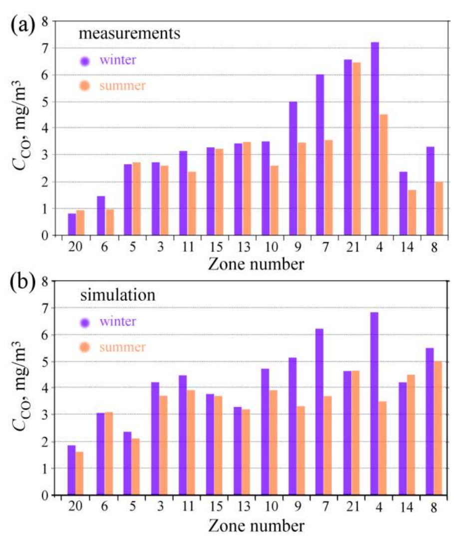

(Hrebtov & Hanjalić, Atmosphere, 2019)

28

Winter diurnal cycle in the City of Sarajevo (TRANS–ASFM)

The Valley: Thermal plumes at noon, colored by vertical velocity (*Žilić 2015*)

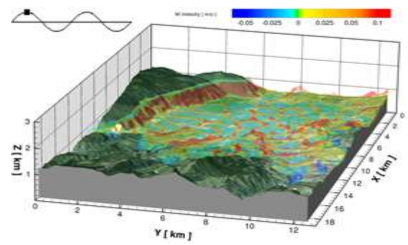

Wind around high-rise buildings, colour: streamwise vel. at *z*=2m (*Bevrnja et al. 2015*)

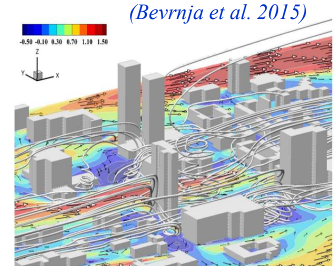

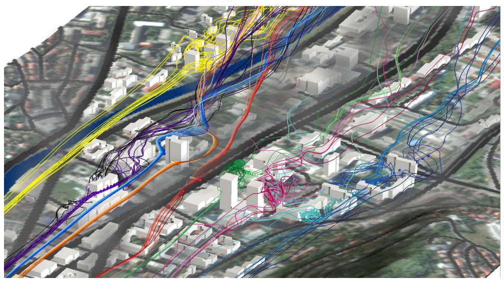

Streamlines and smog at 08:00h.

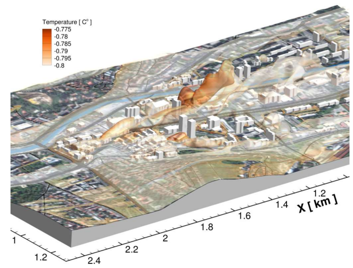

Relative concentration C/C_0=0.5‰ (traffic emission) colored by temperature

29

Buoyancy-driven microclimate phenomena: OUTLOOK

- LES & DNS will continue to be the main research tool for gaining insight into the physics; → irregular domains, larger grids (≥10^9), *but*
  - 'Having terabytes of data at disposal greatly increases the chances that you will find the answer to even the toughest questions – if you don't mind searching for a needle in a giant digital haystack' (*Ehrenman, 2005*)
- For real-life configurations, URANS will prevail as the rational tool provided specific issues are accounted for (ground/wall b. c., intrinsic unsteadiness, organised structures, counter-gradient diffusion,….) (e.g. T-RANS ASFM k–ε–θ^2 with buoyancy-accounting NE G/WF…)
- *For real* urban canopies, more advanced (U)RANS needed: e.g. Elliptic-relaxation and blending with LES (Hybrid RANS-LES)
- The above apply equally to *engineering* and *industrial flows* in complex settings driven by thermal buoyancy at high Ra No's.

"The test of science is its ability to predict". (*R. Feynman 1977*)

30